

Facile Preparation of Mn-doped CeO₂ Submicrorods by Composite-Hydroxide-Salt-Mediated Approach and Their Magnetic Property

Jie Tan*, Wei Zhang, Yao-Hui Lv, Ai-Lin Xia

Anhui Key Laboratory of Metal Materials and Processing, School of Materials Science and Engineering, Anhui University of Technology, Anhui, Maanshan 243002, P.R. China

Received: June 27, 2012; Revised: October 17, 2012

Mn-CeO₂ submicrorods have been obtained from anomalous CeO₂ particles through a novel composite-hydroxide-salt-mediated (CHSM) approach. This method is based on a reaction between a metallic salt and a metallic oxide in a solution of composite-hydroxide-salt eutectic at ~225 °C and normal atmosphere without using an organic dispersant or capping agent. The magnetic measurement of the Mn-CeO₂ submicrorods exhibits an enhanced ferromagnetic property at room temperature with a remanence magnetization (M_r) of 1.4×10^{-3} emu.g⁻¹ and coercivity (H_c) of 75 Oe. The UV-visible spectra reveal that the absorption peak of the CeO₂ shifts from ultraviolet region to visible light region after being doped with Mn ions. The room temperature ferromagnetic properties and light absorption of the Mn-CeO₂ submicrorods would have wide applications in spintronics and photocatalysis field.

Keywords: Mn-CeO₂ submicrorods, crystal growth, morphology, magnetic properties

1. Introduction

Ceria (CeO₂) is an ionic and insulating oxide with the cubic fluorite structure (CaF₂). It has been widely used in fuel cells^{1,2}, treatment of industrial wastewater³⁻⁵. In addition, they have been used as polishing media in optics⁶, as components for H₂ production⁷ and as efficient catalysts⁸. More recently, ceria doped with metal ions has exhibited novel properties in many aspects. Xia et al.⁹ have prepared Mn-doped CeO₂ nanorods by facile composite-hydroxide-mediated (CHM) approach. They suggested that Mn-doped CeO₂ nanorods would have potential applications in photocatalysis and building of photovoltaic devices. R.S. de Biashi et al.¹⁰ have investigated electron spin resonance spectra of Cu²⁺ in diluted solid solutions of Cu in CeO₂. The results suggest that the solid solution of Cu in CeO₂ exhibits clustering effects. Copper-doped CeO₂ is used as a catalyst, especially for the reduction of SO₂ by CO¹¹⁻¹³. G. Qi et al.¹⁴⁻¹⁵ have reported the application of Mn-CeO₂ in the low-temperature selective catalytic reduction (SCR) of NO_x. Corma et al.¹⁶ found that CeO₂ nanoparticles as well as rare-earth-doped ceria did not need photosensitization to have photovoltaic activity in the visible region. Wen et al.¹⁷ have found that the absorption coefficient of Fe-CeO₂ in a frequency range of 0.2-1.8 THz was less than 0.35 cm⁻¹. The result indicates that Fe-CeO₂ may be a potential candidate as THz optical materials. Chen et al.¹⁸ have investigated the synthesis and room-temperature ferromagnetism of CeO₂ nanocrystals with nonmagnetic Ca²⁺ doping (Ca-CeO₂). Zhang et al.¹⁹ have synthesized Ba-doped CeO₂ nanowires and found

that their humidity sensitivity was greatly enhanced in comparison with pure CeO₂ particles. Additionally, Gd-, Sm-, Y-, Tb- and Fe-doped CeO₂ have been studied extensively²⁰⁻²⁴.

In the current research, we report a novel approach for the synthesis of Mn-CeO₂ submicrorods. The method is based on a reaction between a metallic salt and a metallic oxide in a solution of molten mixed potassium nitrate and potassium hydroxide eutectic at ~225 °C and normal atmosphere without using an organic dispersant or capping agent. Although the melting points (T_m) of both pure potassium hydroxide and potassium nitrate are over 300 °C, $T_m = 404$ °C for KOH and $T_m = 337$ °C for KNO₃, the eutectic point at KOH/KNO₃ = 63.8:36.2 is only about 225 °C. During the reaction process, hydroxides work not only as the solvent but also as the reactant for reducing the reaction temperature. The advantage of this methodology is the easy recycle of by-products, owing to applying the salt nitrate and hydroxide of the same metal. Additionally, this methodology provides a one-step, convenient, low-cost, nontoxic, and mass-production route for the synthesis of nanostructures of functional oxide materials.

The as-synthesized submicrorods were characterized by X-ray diffraction (XRD), scanning electron microscopy (SEM), transmission electron microscopy (TEM). The magnetic properties of the Mn-CeO₂ submicrorods were investigated. Photoabsorption of Mn-CeO₂ submicrorods and pure CeO₂ particles were comparatively studied via UV-visible diffuse reflectance spectra.

*e-mail: tanjie@ahut.edu.cn

2. Experimental

Mn-CeO₂ submicrorods were synthesized by the composite-hydroxide-salt-mediated (CHSM) method without using any capping agent. All reactants were of analytical grade. The synthesis steps are as follows: (1) a total of 20 g of KOH and KNO₃ was mixed at a ratio of 63.8:36.2 and placed in a 25 mL Teflon vessel. (2) A mixture of 1 mmol CeO₂ and 1 mmol Mn(NO₃)₂·6H₂O each was used as the raw material for reaction, and was placed on the top of the hydroxide and salt nitrate in the vessel. (3) The Teflon vessel was put into a furnace preheated to 235 °C. (4) After the hydroxide and salt nitrate were totally molten (30 minutes later), the molten reactants were mixed uniformly by shaking the covered vessel. (5) 24 hours later, the vessel was taken out and cooled to room temperature naturally. The product was collected by centrifugation and through washing with deionized water and ethanol.

X-ray diffraction measurement (XRD, D8-Advance, Germany) with the use of Cu K α radiation ($\lambda = 1.5418 \text{ \AA}$) in the 2θ range from 20° to 70° were used to investigate the crystal phase. The morphology and the size of the synthesized samples were characterized by a field emission scanning electron microscopy (SEM, S-4800, Japan) and at 120 kV by a transmission electron microscopy (TEM, JEM-100CXII, Japan). Energy-dispersive spectroscopy (EDS) was employed to determine the final actual Mn concentration in the composites. The selected-area diffraction (SAED) pattern was taken on the TEM. Ultraviolet-visible (UV-vis) diffuse reflectance spectra were obtained for the dry-pressed disk samples by using a Shimadzu UV-2550 recording spectrophotometer, which was equipped with an integrating sphere, and BaSO₄ was used as a reference. The magnetic measurement was obtained on a Micromag Model 2900 Alternating Gradient Magnetometer (AGM). The magnetic hysteresis loop was observed in the range of $-10 \text{ kOe} < H < 10 \text{ kOe}$ at temperature of 293 K.

3. Results and Discussion

Figure 1 shows the XRD patterns of the source material CeO₂ and the Mn-CeO₂ sample synthesized at 235 °C for 24 hours. All the peaks are assigned by using the JCPDS file (no. 34-0394) which is a pure cubic phase (*Fm3m*). Comparing the curves of the pure CeO₂ with that of the Mn-CeO₂ submicrorods, there are no additional diffraction peaks, indicating that Mn ions might have entered into the CeO₂ lattices and there are no secondary phases or precipitates in the Mn-CeO₂ sample. Additionally, we also find that diffraction peaks of the Mn-CeO₂ submicrorods slightly shift to larger Bragg angles. One possible explanation might be that the incorporation of Mn²⁺ or Mn³⁺ into the lattice results in the decrease of the lattice parameters as the ionic radius of Mn²⁺ (0.066 nm) and Mn³⁺ (0.062 nm) are smaller than that of Ce⁴⁺ (0.097 nm)⁹.

Figure 2a, c shows the SEM images of the source material CeO₂ and the Mn-CeO₂ submicrorods, respectively. The anomalous particles morphology of the source material CeO₂ can be seen with the diameter ranging from 2-8 μm . When doped with Mn ions, the particles convert gradually

into submicrorods with lengths of 2-3 μm , as shown in Figure 2b. For Mn-CeO₂ submicrorods, the crystal face is clean and sharp, and no amorphous layer is present, because no organic reagent of capping material was introduced during the synthesis process. The interesting morphological conversion of the CeO₂ from anomalous particles into single-crystal submicrorods might be explained by a dissolution-recrystallization mechanism²⁵. The crystal growth experiences first the CeO₂ and Mn(NO₃)₂ dissolving in the molten composite alkali and salt of the same metal solvent, and then CeO₂ recrystallizing while some Mn ions dope in, and finally crystal growth into the submicrorod morphology. The selected area electron diffraction (SAED) pattern of the corresponding edge of the submicrorod in Figure 2b demonstrates its single-crystalline structure. The growth direction of the submicrorods is [110]. The EDS indicates the existence of Ce, Mn and O in the submicrorods (Figure 2d). In addition, EDS measurement shows that the ratio of the elements in the product is Mn/Ce/O = 1:1:4, demonstrating the controllability in chemical composition.

The XPS measurements provided further information for the evaluation of the purity and surface composition of the Mn doped CeO₂ sample. The XPS survey spectrum in Figure 3a demonstrates no peaks of other elements than C, Mn, Ce and O in the sample. Figure 3b-d shows the high-resolution XPS spectra of Ce 3d, Mn 2p and O 1s, respectively. Figure 3b illustrates Ce 3d XPS spectra measured for the Mn doped CeO₂ samples. The six components observed in the spectrum (882.7, 889.1, 898.6, 900.9, 907.9 and 916.7 eV) could be assigned unambiguously to Ce⁴⁺ species by comparison with data reported in the literature²⁶. The two peaks of the Mn region at 640.8 eV and 652.7 eV are assigned to Mn 2p_{3/2} and Mn 2p_{1/2}, demonstrating the existence of Mn²⁺^[27]. The O 1s peak centered at 529.3 eV belongs to the O²⁻ in Ce-O bond⁹.

Figure 4 shows the UV-visible diffuse reflectance spectra of the raw material CeO₂ (Figure 4a) and the as-synthesized Mn-CeO₂ submicrorods (Figure 4b). From this figure, we observe that the absorption peak is in the visible light region centered at 414.5 nm after being doped with Mn ions. Xia et al.⁹ have reported that the absorption peak of CeO₂ and Mn-CeO₂ submicrorods was in the ultraviolet region centered at 349.22 nm and the visible light region centered at 403.96 nm, respectively. Thurber et al.²⁸ have reported the similar phenomenon of the Ni-doped CeO₂. They found that the band gap changed from 3.80 to 3.23 eV when the CeO₂ was doped with 4% Ni. Thurber et al. attributed this change to the extensive structural changes caused by the incorporation of interstitial Ni. Xia et al. speculated that the peak shift was the result of the defects (such as oxygen vacancies) or the impurities caused from the incorporation of the Mn ions as the defects and impurities could result in the formation of sublevels within the band gap. In conclusion, the red-shift phenomenon has been observed in this experiment which could be attributed to electron-phonon coupling. In certain systems, electron-phonon coupling could be strong enough to overcome the spatial confinement to determine the energy of excitons. It determines or modifies the effective mass of carriers and the style of

carrier scattering by the lattice, leading to a red-shift of the emission band^{29,30}. In addition, we have also observed that the absorption range of the Mn-CeO₂ submicrorods is wider than that of the pure CeO₂ particles. This phenomenon suggests the energy absorption from the charge transition

between multisublevels, and indirectly reveals the existence of both defects and impurities. The broad light absorption of the Mn-CeO₂ submicrorods shows promise in photocatalytic or photovoltaic applications by harvesting solar energy, as demonstrated by the rare-earth-doped ceria in the dye-free solar cell¹⁶.

The magnetization hysteresis (M-H) loops of the Mn-CeO₂ submicrorods at 293 K have been measured, as shown in Figure 5. Room temperature ferromagnetism (weak magnetism) of the pure CeO₂ particles has been observed³¹ in which the ferromagnetism was assumed to limited surface defects of the micron-sized particles. However, after the incorporation of Mn ions, the magnetism of the Mn-CeO₂ submicrorods is greatly enhanced. The magnetization increases almost linearly under an applied magnetic field up to 1000 Oe. Saturated magnetization is not observed even under an applied magnetic field up to 10 kOe. From the hysteresis loop between -2000 and 2000 Oe, the remanence magnetization (M_r) of 1.4 × 10⁻³ emu.g⁻¹ and coercivity (H_c) of 75 Oe was observed in Figure 4b. The magnetic properties of CeO₂ doped with metal ions, such as Co, Ni, Ca ions^{25,32,33} have been suggested to originate from a combination of oxygen vacancies and metal ions doping.

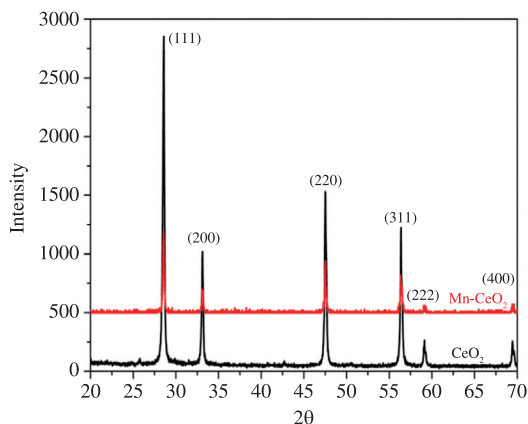


Figure 1. XRD patterns of the source material CeO₂ and the Mn-CeO₂ submicrorods obtained at 235 °C for 24 hours.

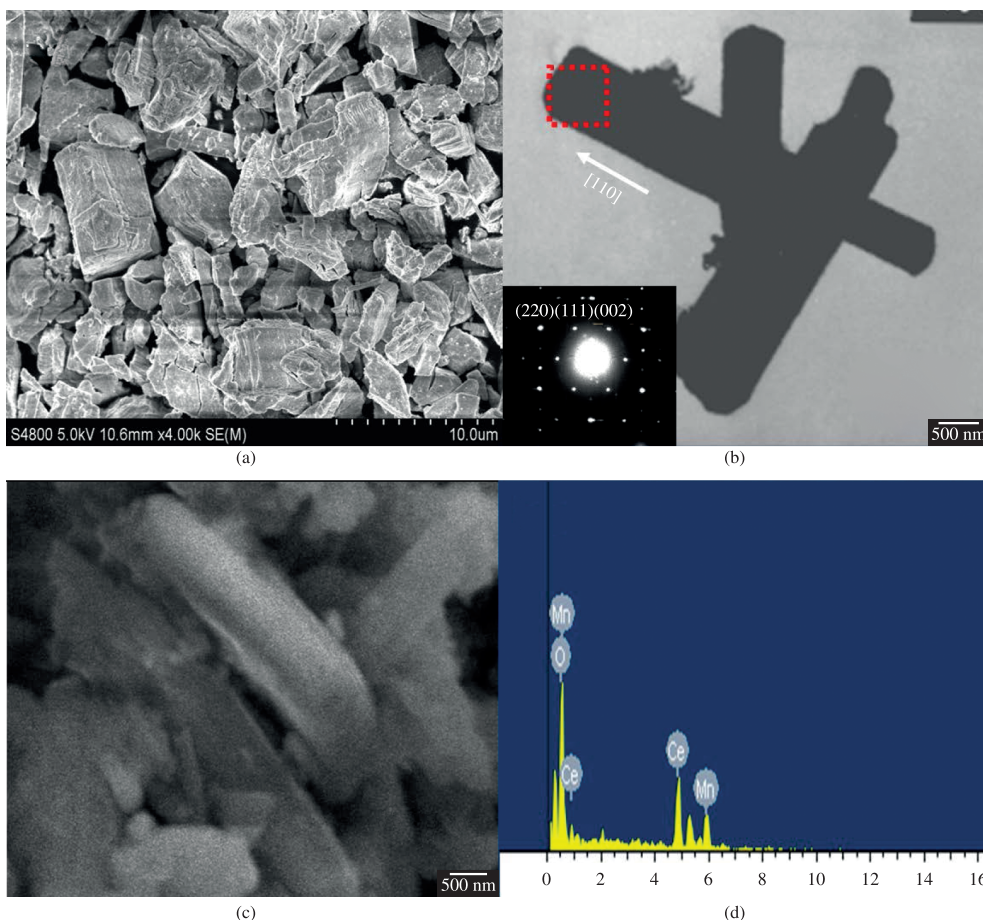


Figure 2. SEM images of the source material CeO₂ (a) and TEM images, electron diffraction pattern (inset of b) of the Mn-CeO₂ submicrorods sample synthesized at 235 °C for 24 hours (b).

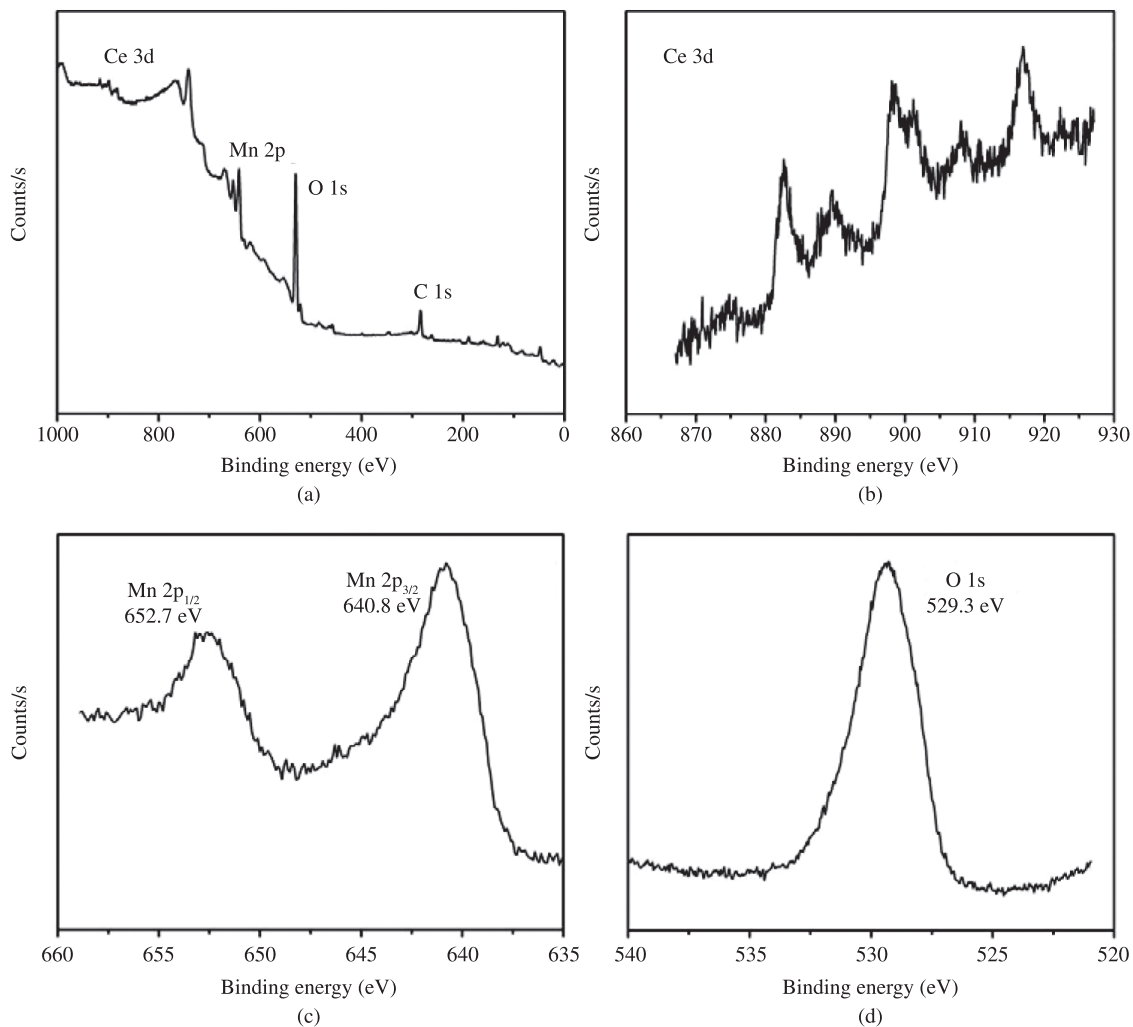


Figure 3. XPS integral spectrum (a) and Ce 3d (b), Mn 2p (c) and O 1s (d) spectrum of Mn-doped CeO₂ nanorods.

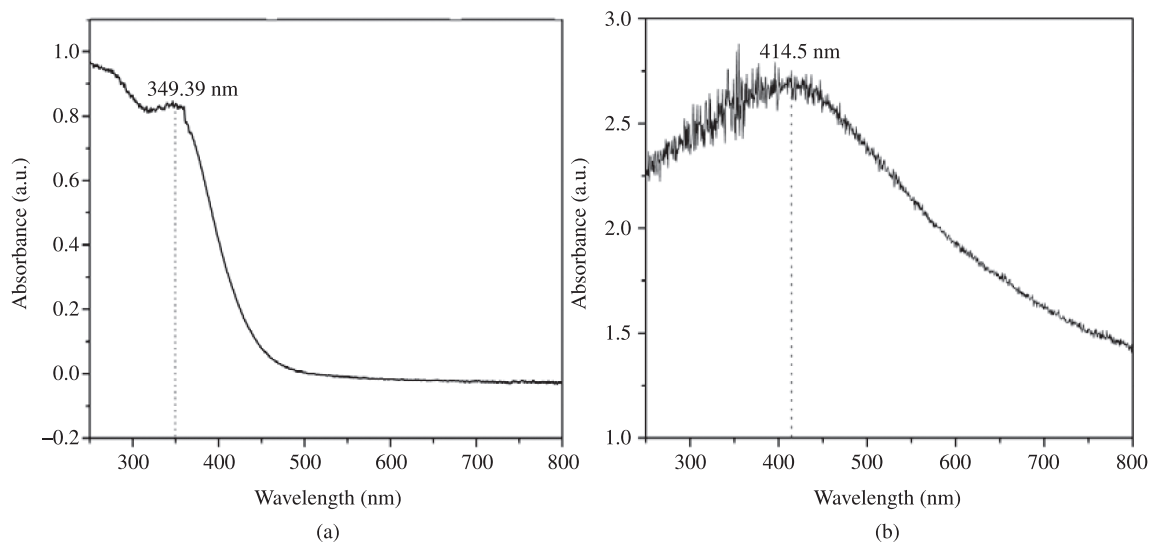


Figure 4. UV-visible diffuse reflectance spectrum of the CeO₂ particles (a) and the Mn-CeO₂ submicrorods (b).

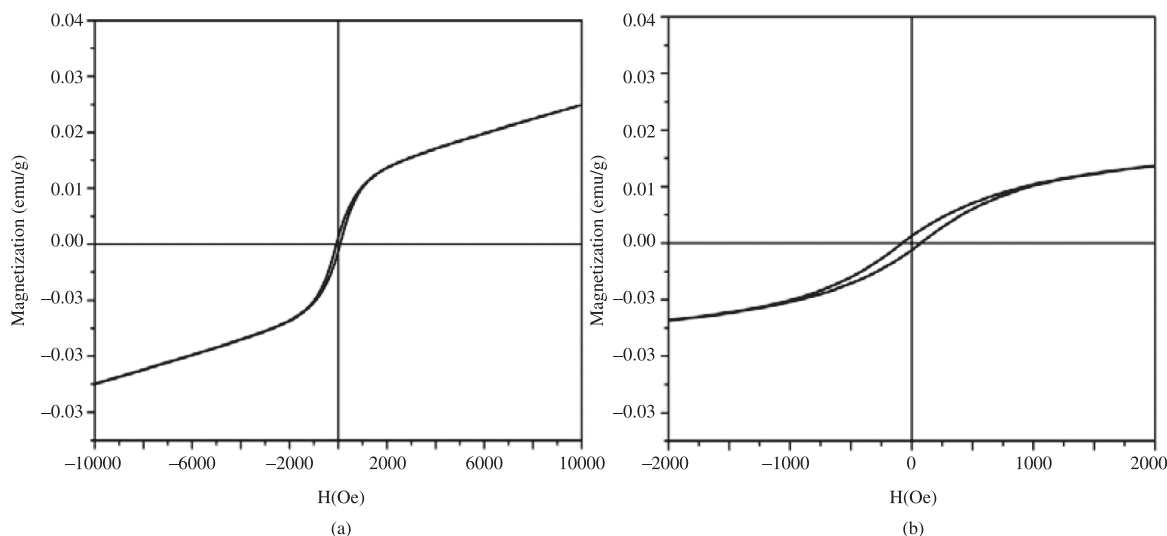


Figure 5. Magnetization hysteresis loop for the obtained Mn-CeO₂ submicrorods at temperature of 293 K.

4. Conclusions

Mn-CeO₂ submicrorods are synthesized from the reaction of CeO₂ with Mn(NO₃)₂·6H₂O through the CHSM method, which provides a one-step, convenient, low-cost, nontoxic, and mass-production route. Owing to the defects and impurities, the absorption spectra of the CeO₂ shows that the peak shifts from the ultraviolet region to the visible light region after being doped with Mn ions. The Mn-CeO₂ submicrorods exhibit an enhanced room temperature ferromagnetism originating from the defects and the doped

Mn ions. The room temperature ferromagnetic properties and light absorption of the Mn-CeO₂ submicrorods suggest potential applications in spintronics and photocatalysis field.

Acknowledgements

The work is financially supported by the Youth Foundation of Anhui University of Technology and The work is financially supported by the National Natural Science Foundation of China (Grant No. 11204003).

References

- Kim CH and Thompson LT. On the importance of nanocrystalline gold for Au/CeO₂ water-gas shift catalysts. *Journal of Catalysis*. 2006; 244:248-250. <http://dx.doi.org/10.1016/j.jcat.2006.08.018>
- Yan M, Mori T, Zou J, Ye F, Ou DR and Drennan J. TEM and XPS analysis of Ca_xCe_{1-x}O_{2-y} (x=0.05-0.5) as electrolyte materials for solid oxide fuel cells. *Acta Materialia*. 2009; 57:722-731. <http://dx.doi.org/10.1016/j.actamat.2008.10.014>
- Nakajima A, Kobayashi T, Isobe T and Matsushita S. Preparation and visible-light photocatalytic activity of Au-supported porous CeO₂ spherical particles using templating. *Materials Letters*. 2011; 65:3051-3054. <http://dx.doi.org/10.1016/j.matlet.2011.06.051>
- Sabari Arul N, Mangalaraj D, Chen PC, Ponpandian N and Viswanathan C. Self assembly of Co doped CeO₂ microspheres from nanocubes by hydrothermal method and their photodegradation activity on AO7. *Materials Letters*. 2011; 65:3320-3322. <http://dx.doi.org/10.1016/j.matlet.2011.07.017>
- Ji PF, Zhang JL, Chen F and Anpo M. Study of adsorption and degradation of acid orange 7 on the surface of CeO₂ under visible light irradiation. *Applied Catalysis B: Environmental*. 2009; 85:148-154. <http://dx.doi.org/10.1016/j.apcatb.2008.07.004>
- Kosynkin VD, Arzgatkina AA, Ivanov EN, Chtoutsa MG, Grabko AI, Kardapolov AV et al. The study of process production of polishing powder based on cerium dioxide. *Journal of Alloys and Compounds*. 2000; 421-425:303-304.
- Abanandes S, Legal A, Cordier A, Peraudeau G, Flamant G and Julbe A. Investigation of reactive cerium-based oxides for H₂ production by thermochemical two-step water-splitting. *Journal of Materials Science*. 2010; 45:4163-4173. <http://dx.doi.org/10.1007/s10853-010-4506-4>
- Qiao DS, Lu GZ, Mao DS, Guo Y and Guo YL. Effect of Ca doping on the performance of CeO₂-NiO catalysts for CH₄ catalytic combustion. *Journal of Materials Science*. 2011; 46:641-647. <http://dx.doi.org/10.1007/s10853-010-4786-8>
- Xia CH, Hu CG, Chen P, Wan BY, He XS and Tian YH. Magnetic properties and photoabsorption of the Mn-doped CeO₂ nanorods. *Materials Research Bulletin*. 2010; 45:794-798. <http://dx.doi.org/10.1016/j.materresbull.2010.03.015>
- De Biasi RS and Grillo MLN. Evidence for clustering in Cu²⁺-doped CeO₂. *Journal of Alloys and Compounds*. 2008; 462:15-18. <http://dx.doi.org/10.1016/j.jallcom.2007.08.039>
- Kacimi S, Barbier Junior J, Taha R and Duprez D. Oxygen storage capacity of promoted Rh/CeO₂ catalysts. Exceptional behavior of RhCu/CeO₂. *Catalysis Letters*. 1993; 22:343-350. <http://dx.doi.org/10.1007/BF00807243>
- TschÖpe AS, Liu W, Flytzani-Stephanopoulos M and Ying JY. Redox activity of nanostochiometric cerium oxide-based nanocrystalline catalysts. *Journal of Catalysis*. 1995; 157:42-50. <http://dx.doi.org/10.1006/jcat.1995.1266>

13. Rodriguez JA, Jirsak T, Freitag A, Hanson JC, Lares JZ and Chaturvedi S. Interaction of SO_2 with CeO_2 and Cu/CeO_2 catalysts: photoemission, XANES and TPD studies. *Catalysis Letters*. 1999; 62:113-119. <http://dx.doi.org/10.1023/A:1019007308054>
14. Qi G and Yang RT. Performance and kinetics study for low-temperature SCR of NO with NH_3 over $\text{MnO}_x\text{-CeO}_2$ catalyst. *Journal of Catalysis*. 2003; 217:434-441.
15. Qi G and Yang RT. Characterization and FTIR studies of $\text{MnO}_x\text{-CeO}_2$ catalyst for low-temperature selective catalytic reduction of NO with NH_3 . *The Journal of Physical Chemistry B*. 2004; 108:15738-15747. <http://dx.doi.org/10.1021/jp048431h>
16. Corma A, Atienzar P, Garc H and Chane-Ching JY. Hierarchically mesostructured doped CeO_2 with potential for solar-cell use. *Nature Materials*. 2004; 3:394-397. <http://dx.doi.org/10.1038/nmat1129>
17. Wen QY, Zhang HW, Yang QH, Li S, Xu DG and Yao JQ. Fe-doped polycrystalline CeO_2 as terahertz optical material. *Chinese Physics Letters*. 2009; 26:047803. <http://dx.doi.org/10.1088/0256-307X/26/4/047803>
18. Chen XB, Li GS, Su YG, Qiu XQ, Li LP and Zou ZG. Synthesis and room-temperature ferromagnetism of CeO_2 nanocrystals with nanomagnetic Ca^{2+} doping. *Nanotechnology*. 2009; 20:115606. <http://dx.doi.org/10.1088/0957-4484/20/11/115606>
19. Zhang ZW, Hu CG, Xiong YF, Yang RS and Wang ZL. Synthesis of Ba-doped CeO_2 nanowires and their application as humidity sensors. *Nanotechnology*. 2007; 18:465504. <http://dx.doi.org/10.1088/0957-4484/18/46/465504>
20. Ye F, Mori T, Ou DR, Takahashi M, Zou J and Drennan J. Ionic conductivities and microstructure of ytterbium doped ceria. *Journal of the Electrochemical Society*. 2007; 154: B180-B185. <http://dx.doi.org/10.1149/1.2403084>
21. Ou DR, Mori T, Ye F, Zou J and Drennan J. Evidence of intragranular segregation of dopant cations in heavily yttrium-doped ceria. *Electrochemical and Solid-State Letters*. 2007; 10:1-3. <http://dx.doi.org/10.1016/j.ssi.2004.09.046>
22. Mori T, Wang YR, Drennan J, Auchterlonie G, Li JG and Ikegami T. Influence of particle morphology on nano-structural feature and conducting property in Sm-doped CeO_2 sintered body. *Solid State Ionics*. 2004; 175:641-649. <http://dx.doi.org/10.1016/j.ssi.2004.09.046>
23. Mori T, Drennan J, Wang YR, Auchterlonie G, Li JG and Yago A. Influence of nano-structural feature on electrolytic properties in Y_2O_3 doped CeO_2 system. *Science and Technology of Advanced Materials*. 2003; 4:213-220. [http://dx.doi.org/10.1016/S1468-6996\(03\)00047-0](http://dx.doi.org/10.1016/S1468-6996(03)00047-0)
24. Zhang TS, Hing P, Huang HT and Kilner J. Early-stage sintering mechanisms of Fe-doped CeO_2 . *Journal of Materials Science*. 2002; 37:997-1003. <http://dx.doi.org/10.1023/A:1014362000128>
25. Lu J, Xie Y, Xu F and Zhu LY. Study of the dissolution behavior of selenium and tellurium in different solvents—a novel route to Se, Te tubular bulk single crystals. *Journal of Materials Chemistry*. 2002; 12:2755-2761. <http://dx.doi.org/10.1039/b204092a>
26. Shuyu JZ, Otto K, Watkins WLH, Graham GW, Belitz RK and Gandhi HS. Characterization of Pd/ γ -alumina catalysts containing ceria. *Journal of Catalysis*. 1988; 114:23-33. [http://dx.doi.org/10.1016/0021-9517\(88\)90005-X](http://dx.doi.org/10.1016/0021-9517(88)90005-X)
27. Wu XD, Liang Q, Weng D, Fan J and Ran R. Synthesis of $\text{CeO}_2\text{-MnO}_x$ mixed oxides and catalytic performance under oxygen-rich condition. *Catalysis Today*. 2007; 126:430-435. <http://dx.doi.org/10.1016/j.cattod.2007.06.014>
28. Thurber A, Reddy KM, Shutthanandan V, Engelhard MH, Wang C, Hays J et al. Ferromagnetism in chemically synthesized CeO_2 nanoparticles by Ni doping. *Physical Review B*. 2007; 76:165206-165213. <http://dx.doi.org/10.1103/PhysRevB.76.165206>
29. Zou BS, Xiao LZ, Li TJ, Zhao JL, Lai ZY and Gu SW. Absorption redshift in TiO_2 ultrafine particles with surfacial dipole layer. *Applied Physics Letters*. 1991; 59:1826-1828. <http://dx.doi.org/10.1063/1.106211>
30. Lu XW, Li XZ, Chen F, Ni CY and Chen ZG. Hydrothermal synthesis of prism-like mesocrystal CeO_2 . *Journal of Alloys and Compounds*. 2009; 476:958-962. <http://dx.doi.org/10.1016/j.jallcom.2008.09.198>
31. Anwar MS, Kumar S, Ahmed F, Arshi N, Kil GS, Park DW et al. Hydrothermal synthesis and indication of room temperature ferromagnetism in CeO_2 nanowires. *Materials Letters*. 2011; 65:3098-3101. <http://dx.doi.org/10.1016/j.matlet.2011.06.042>
32. Wen QY, Zhang HW, Song YQ, Yang QH, Zhu H and Xiao JQ. Room-temperature ferromagnetism in pure and Co doped CeO_2 powders. *Journal of Physics: Condensed Matter*. 2007; 19:246205-246211. <http://dx.doi.org/10.1088/0953-8984/19/24/246205>
33. Song YQ, Zhang HW, Wen QY, Zhu H and Xiao JQ. Co doping effect on the magnetic properties of CeO_2 films on Si (111) substrates. *Journal of Applied Physics*. 2001; 102:043912-043916. <http://dx.doi.org/10.1063/1.2761847>